Biochimica et Biophysica Acta 1864 (2016) 1195–1205

Contents lists available at ScienceDirect

Biochimica et Biophysica Acta

journal homepage: www.elsevier.com/locate/bbapap

Caenorhabditis elegans AGXT-1 is a mitochondrial and temperature-adapted ortholog of peroxisomal human AGT1: New insights into between-species divergence in glyoxylate metabolism

Noel Mesa-Torres [a,*,1], Ana C. Calvo [b,1], Elisa Oppici [c], Nicholas Titelbaum [a,b], Riccardo Montioli [c], Antonio Miranda-Vizuete [d], Barbara Cellini [c], Eduardo Salido [e], Angel L. Pey [a,*]

[a] Department of Physical Chemistry, Faculty of Sciences, University of Granada, Av. Fuentenueva s/n, 18071 Granada, Spain
[b] Program in Cellular Neuroscience, Neurodegeneration, and Repair, Department of Cell Biology, Yale University School of Medicine, New Haven, CT 06536, USA
[c] Department of Neurological, Biomedical and Movement Sciences, Section of Biological Chemistry, University of Verona, Strada Le Grazie 8, 37134 Verona, Italy
[d] Instituto de Biomedicina de Sevilla, Hospital Universitario Virgen del Rocío/Consejo Superior de Investigaciones Científicas/Universidad de Sevilla, 41013 Sevilla, Spain
[e] Centre for Biomedical Research on Rare Diseases (CIBERER), University Hospital of the Canary Islands, and CIBICAN, University of La Laguna, 38320 Tenerife, Spain

ARTICLE INFO

Article history:
Received 13 January 2016
Received in revised form 27 April 2016
Accepted 10 May 2016
Available online 11 May 2016

Keywords:
Primary hyperoxaluria
Enzyme kinetics
Substrate specificity
Protein stability
Conformational disease

ABSTRACT

In humans, glyoxylate is an intermediary product of metabolism, whose concentration is finely balanced. Mutations in peroxisomal alanine:glyoxylate aminotransferase (hAGT1) cause primary hyperoxaluria type 1 (PH1), which results in glyoxylate accumulation that is converted to toxic oxalate. In contrast, glyoxylate is used by the nematode *Caenorhabditis elegans* through a glyoxylate cycle to by-pass the decarboxylation steps of the tricarboxylic acid cycle and thus contributing to energy production and gluconeogenesis from stored lipids. To investigate the differences in glyoxylate metabolism between humans and *C. elegans* and to determine whether the nematode might be a suitable model for PH1, we have characterized here the predicted nematode ortholog of hAGT1 (AGXT-1) and compared its molecular properties with those of the human enzyme. Both enzymes form active PLP-dependent dimers with high specificity towards alanine and glyoxylate, and display similar three-dimensional structures. Interestingly, AGXT-1 shows 5-fold higher activity towards the alanine/glyoxylate pair than hAGT1. Thermal and chemical stability of AGXT-1 is lower than that of hAGT1, suggesting temperature-adaptation of the nematode enzyme linked to the lower optimal growth temperature of *C. elegans*. Remarkably, *in vivo* experiments demonstrate the mitochondrial localization of AGXT-1 in contrast to the peroxisomal compartmentalization of hAGT1. Our results support the view that the different glyoxylate metabolism in the nematode is associated with the divergent molecular properties and subcellular localization of the alanine:glyoxylate aminotransferase activity.

1. Introduction

Glyoxylate is an intermediary product of metabolism in humans, which is formed from precursors such as glycine, glycolate, hydroxypyruvate and hydroxyproline. Among mammals, alanine:glyoxylate aminotransferase (AGT) protein compartmentalization is linked to metabolism of glyoxylate precursors, varying from mainly mitochondrial in carnivorous, peroxisomal in herbivorous and located in both organelles in omnivorous [1]. The human *AGXT* gene encodes an alanine:glyoxylate aminotransferase enzyme (hAGT1; E.C. 2.6.1.44) that is responsible for glyoxylate detoxification in peroxisomes of hepatocytes [2] thus balancing the glyoxylate concentration. The human genome encodes a second protein with alanine:glyoxylate aminotransferase activity named hAGT2 [3] that catalyses multiple aminotransferase reactions [4,5] and might be involved in the metabolism of glyoxylate within the mitochondria. hAGT1 is a pyridoxal 5′-phosphate (PLP)-dependent enzyme that catalyses the amino transfer from L-alanine to glyoxylate resulting into pyruvate and glycine and this reaction is largely shifted towards glycine formation [6]. Mutations in *AGXT* gene cause primary hyperoxaluria type 1 (PH1), an error of amino acid metabolism inherited in an autosomal recessive manner [2]. PH1 results in the accumulation of glyoxylate in hepatocytes where it is oxidized to oxalate (a metabolic-end product in humans) causing progressive renal failure and ultimately leading to a build-up of oxalate and life-threatening oxalate precipitation [2,7]. Currently, the best method to treat PH1 is a double liver and kidney transplantation, but this treatment often shows significant rates of morbidity and mortality.

After the complete sequencing of *Caenorhabditis elegans* genome, early estimations indicated that around 74% of human gene sequences had nematode counterparts [8]. Therefore, a lot of effort was put into identifying potential nematode orthologs to human genes. As a result,

* Corresponding authors.
E-mail addresses: noelmesatorres@gmail.com (N. Mesa-Torres), angelpey@ugr.es (A.L. Pey).
[1] These authors contributed equally to this work.

http://dx.doi.org/10.1016/j.bbapap.2016.05.004
1570-9639/

using an *in silico* search of genes associated with inborn errors of metabolism in humans, an open-reading frame termed as *T14D7.1* was predicted as an ortholog of human *AGXT* gene [9]. The *T14D7.1* gene (now renamed as *agxt-1*) is located on chromosome 2 and it is organized into 11 exons (WBGene00011767), whose conceptual translation results into a 405 amino acids protein (AGXT-1). Unlike humans, the nematode *C. elegans* has an active glyoxylate cycle (GC) [10] that allows to bypass the decarboxylation steps of the tricarboxylic acid (TCA) cycle [11], thus linking catabolic and biosynthetic capacities. In the nematode, the key enzyme of this cycle is a single bi-functional enzyme (ICL-1), which has isocitrate lyase activity (N-terminal domain) and malate synthase activity (C-terminal domain) [12] that are regulated in a developmentally specific manner [13,14].

We herein present data supporting that the divergent glyoxylate metabolism between humans and the nematode *C. elegans* could involve different molecular properties and subcellular localization of their respective AGT enzymes. Further, we demonstrate that even though AGXT-1 and hAGT1 proteins have similar quaternary structure and substrate specificities, AGXT-1 displays higher specific activity and lower protein stability, possibly reflecting temperature adaptation of the nematode enzyme. *In vivo* studies demonstrate the mitochondrial localization of AGXT-1 in contrast to the peroxisomal functional environment of hAGT1. In this work, we provide novel insights into the evolutionary changes in protein stability, roles of AGT proteins and the divergence of glyoxylate metabolism between vertebrates and invertebrates.

2. Materials and methods

2.1. C. elegans AGXT-1 cloning, expression and purification

The *agxt-1* ORF was amplified from a *C. elegans* cDNA library and cloned into a pET-28 (Novagen) vector using the primers ACA**GCTAGC**ATGCAGCCAACAGGGAATCAAATA and TAT**GTCGAC**TTAA-ACCAAATTAGGATCCGATGGACTT forward and reverse respectively and restriction enzymes *Nhe*I-HF and *Sal*I-HF (New England Biolabs). This construct incorporates a His-tag sequence at the N-terminal domain of AGXT-1. *E. coli* BL21(DE3) competent cells were transformed with the plasmid and were grown in LB medium supplemented with 30 $\mu g \cdot ml^{-1}$ kanamycin. Overnight cultures were diluted 40-fold in fresh LB-kanamycin for 3 h at 37 °C and induced at 4 °C by adding IPTG 0.5 mM for 8 h. Cells were harvested and lysed by sonication in binding buffer (20 mM NaH_2PO_4, 200 mM NaCl, 50 mM imidazole, pH 7.4) supplemented with protease inhibitors (EDTA-free protease inhibitor cocktail, Roche). Soluble extracts obtained after ultracentrifugation at 70,000 × *g* were loaded onto an IMAC columns (GE Healthcare) and eluted with binding buffer supplemented with 500 mM imidazole. His-AGXT-1 was further purified by size exclusion chromatography using a HiLoad™ 16/60 Superdex™ 200 column running in 20 mM Hepes (2-[4-(2-hydroxyethyl)piperazin-1-yl]ethanesulfonic acid), 200 mM NaCl, pH 7.4. The concentration of His-AGXT-1 (hereafter AGXT-1) protein was evaluated using a sequence-based extinction coefficient of 0.763 ml mg^{-1} cm^{-1} at 280 nm [15]. The purification of hAGT1 was performed as described previously [16]. Isolation of apo-forms of both enzymes was attempted by using the protocol previously described [17]. PLP concentration was calculated by using a molar extinction coefficient of 4900 M^{-1} cm^{-1} at 388 nm [18].

2.2. Spectroscopic analyses

All the spectroscopic assays were performed in a 20 mM Hepes, 200 mM NaCl, pH 7.4 buffer at 25 °C. UV–visible absorption spectroscopy was performed in an Agilent 8453 diode-array spectrophotometer using cuvettes with a path length of 3 mm and 20 μM protein (in subunit). Near-UV/visible circular dichroism measurements were performed in a Jasco J-710 spectropolarimeter by using 5-mm path length cuvettes with 20 μM protein (in subunit). Dynamic light scattering was carried out using a protein concentration of 5 μM (in subunit) in the presence of 50 μM PLP in a Zetasizer Nano ZS (Malvern Inc.) with 3-mm path length cuvettes and applying the Stokes–Einstein equation assuming a spherical shape for the scattering particles.

2.3. Enzyme activity measurements

The overall transaminase activity was measured at 37 °C with a protein concentration of 2.5 $\mu g \cdot ml^{-1}$ in the presence of 150 μM PLP in 0.1 M phosphate buffer pH 8. The time of the reaction was 2 min and the substrate concentration was 0.25–2 mM glyoxylate and 0–100 mM L-alanine. Pyruvate formation was evaluated following the oxidation of NADH at 340 nm by a coupled enzyme assay using lactate dehydrogenase [19] during 3 min at 37 °C. Global fittings were performed according to double-displacement mechanisms [6,16]. To determine the pH dependence, activity measurements were performed using this coupled assay in the presence of 2 mM glyoxylate and 100 mM L-alanine at 37 °C in the following buffers: 100 mM Hepes (pH 7–8), MES (2-(N-morpholino)ethanesulfonic acid, pH 6–6.5), acetate (pH 4.5–5.5) or formiate (pH 3–4). The time of the transamination reaction was set at 1.5 min (pH 7–8), 4 min (pH 6–6.5) and 10 min (pH 3.5–5-5). The dependence of specific activity on temperature was measured at 15, 20, 25, 30 and 37 °C with reaction times from 2 to 10 min. To investigate the substrate specificity, the overall transamination reaction was measured in the presence of different amino acids (L-alanine, L-serine, L-arginine, L-glutamate, L-aspartate and L-phenylalanine) and ketoacids (glyoxylate and pyruvate) by incubating the enzymes (2.5–100 $\mu g \cdot ml^{-1}$) with the amino acid at 100 mM, the ketoacid at 2 mM and in the presence of 200 μM PLP in 0.1 M phosphate buffer, pH 8 and 37 °C. Aliquots of each reaction mixture were collected at various times and the reaction was stopped by adding 10% (*w*/*v*) trichloroacetic acid. The amount of ketoacid consumed was determined by HPLC after derivatization with 2.4-dinitrophenylhydrazine as previously described [20].

2.4. Differential scanning calorimetry

DSC experiments were performed and analysed as previously described for hAGT1 [17,21]. Briefly, the model considers the irreversible denaturation of the native protein to a final state that cannot fold back, and this kinetic conversion is characterized by a first-order rate constant *k*, which changes with temperature according to the Arrhenius equation. The half-life at any temperature can thus be obtained from extrapolation of *k* to a given temperature following the Arrhenius plot and determined as $t_{1/2} = \ln(2)/k$.

2.5. Urea denaturation

Urea denaturation of AGXT-1 and hAGT1 was performed by incubating the enzymes (5 μM in protein subunit) in 20 mM Hepes, 200 mM NaCl, 1 mM TCEP (Tris(2-carboxyethyl)phosphine) pH 7.4 with urea at concentrations ranging from 0 to 8 M. Urea concentration was determined by refractive index measurements. Samples were incubated at 25 °C for 16 h and then denaturation was monitored by Far-UV circular dichroism spectroscopy (200–260 nm; 1 mm quartz cuvettes) in a Jasco J-710 spectropolarimeter. Refolding experiments were performed by dilution of protein samples denatured in 8 M urea solution with urea-free buffer and allowed to equilibrate at 25 °C for 4 h prior to Far-UV CD spectroscopic analyses.

2.6. Structural modelling

The structural model of AGXT-1 protein was obtained using the Modeler v9.13 software, the AGXT-1 amino acid sequence and the crystal structure of human hAGT1 (pdb 1H0C) protein as a template.

The model refinement was performed by energy minimization applying the CHARM27 force field of the MOE software. The adjustment of the protonation state, the coordinate based isoelectric point calculation, the electrostatic surface map drawing, the structural alignment and the image construction were performed using MOE 2013 software (CCG group).

2.7. Strains

C. elegans worms were cultured and handled as described before [22]. The following strains were used: wild type N2 Bristol, UGR1 *alpEx1* [*Pmyo-3*::*tomm-20*::*gfp*, *Pmyo-3*::*agxt-1*(*50aa*)::*tagrfp*, *Punc-122*::*gfp*], UGR3 *alpEx3* [*Pmyo-3*::*tomm-20*::*gfp*, *Pmyo-3*::*agxt-1*(*100aa*)::*tagrfp*, *Punc-122*::*gfp*], UGR7 *alpEx7* [*Pmyo-3*::*tomm-20*::*gfp*, *Pmyo-3*::*tagrfp*, *Punc-122*::*gfp*], UGR9 *agxt-1* (*tm6307*), UGR10 *icl-1* (*ok531*), and UGR11 *agxt-1*(*tm6307*); *icl-1* (*ok531*).

2.8. Molecular biology and transgenic lines

The nucleotide sequence corresponding to the first 50 and 100 amino acids of the *agxt-1* cDNA sequence was amplified and cloned into a gateway plasmid pDONR221. These clones were fused in frame with tagRFP (monomeric RFP) and the *unc-54* gene 3-UTR and expressed under the *myo-3* promoter, using the Multi Site Gateway Pro Plus Kit (ThermoFisher, catalogue number 11791-100 and 11789-013). These plasmids were injected at 5 $ng \cdot \mu l^{-1}$ together with a plasmid expressing the mitochondrial fusion construct TOMM-20::GFP under the control of the same *myo-3* promoter (kindly provided by Dr. Marc Hammarlund, Yale University) at 5 $ng \cdot \mu l^{-1}$ and the co-injection marker *Punc-122*::*gfp*. Transgenic animals were generated using standard techniques [23].

2.9. Fluorescence and confocal image acquisition and analysis

Images of fluorescent fusion proteins were taken in live adults *C. elegans* nematodes using a 60× CFI Plan Apo VC, numerical aperture 1.4, oil-immersion objective on an UltraView VoX spinning-disc confocal microscope (PerkinElmer Life and Analytical Sciences). Worms were synchronized 3 days prior to experiment, and first day of adulthood animals were analysed. Animals were immobilized during image acquisition using 10 μM Levamisol (Sigma). Images were analysed using Volocity software (Improvision).

2.10. Glyoxylate and oxalate determination

C. elegans strains N2, UGR9, UGR10 and UGR11 were grown on NGM plates supplemented with 10 mM sodium glyoxylate monohydrate (Sigma). When bacterial food was about to exhaust, mixed stage populations of worms were washed out from the plates with M9 buffer several times to clean the bacteria off and worm pellet were frozen at −80 °C overnight. Thawed pellet were resuspended in 5 volumes of cold 10 mM Hepes and 0.5% CHAPS buffer supplemented with complete protease inhibitor cocktail (Roche) and sonicated. Lysates were centrifuged at 14,000 rpm for 10 min at 4° and supernatants were transferred into a new tube and immediately frozen. To evaluate glyoxylate content, lysates were deproteinized by the addition of 10% (*w*/*v*) trichloroacetic acid and centrifuged at 13,200 *g* for 2 min. The amount of glyoxylate present in supernatant was determined by HPLC analysis after derivatization with 2.4-dinitrophenylhydrazyne as previously described [20]. The total protein content of each lysate was determined before deproteinization by using the Bradford assay. Oxalate content was evaluated by using the Oxalate Quantitative Enzymatic Color Test Kit (Greiner Diagnostic GmbH) following the manufacturer's protocol.

Table 1
Identity and similarity in pairwise sequence alignments of AGXT-1, hAGT1 and hAGT2 proteins. Alignments were carried out using Clustal Omega [32]. GI numbers of protein sequences are: hAGT1-126522481, hAGT2-119576316 and AGXT-1-5824614.

Residues	hAGT1 *vs.* hAGT2	AGXT-1 *vs.* hAGT1	AGXT-1 *vs.* hAGT2
Identical	75 (19%)	167 (41%)	77 (19%)
Similar	112 (28%)	121 (30%)	103 (25%)

3. Results

3.1. AGXT-1 is a mitochondrial protein

According to a protein sequence comparison, *C. elegans* AGXT-1 shows much higher identity/similarity to peroxisomal hAGT1 protein than to mitochondrial hAGT2, which has a different fold (Table 1). The sequence of AGXT-1 is 13 residues longer than hAGT1 and all catalytic residues involved in the binding and stabilization of the coenzyme at the active site are conserved in both proteins (Fig. 1, red highlighted residues) [24]. However, we also found two interesting differences between the two primary sequences (Fig. 1, green highlighted residues). First, the 13 extra residues of AGXT-1 protein are located at the N-terminal domain. Mitochondrial targeting sequences (MTS) usually consist of 20–60 residues in the N-terminal domain that are prone to form an amphipathic alpha helix [25]. Bioinformatics tools, such as MitoProt [26] or TargetP 1.1 Server [27], predict probabilities of 75–85% for the N-terminal domain of AGXT-1 to form a cleavable amphipathic alpha helix consistent with a potential MTS. Second, the AGXT-1 protein lacks the C-terminal tripeptide that constitutes the peroxisomal targeting sequence type 1 (PTS1) required for hAGT1 peroxisomal import through Pex5p-dependent route [28,29], which is conserved between humans and nematodes [30]. *C. elegans* also lacks the alternative PTS2 pathway to target proteins to peroxisomes [31]. All together, these data suggest that AGXT-1 is not likely to be imported to peroxisomes, in contrast to hAGT1 [2], but more likely to be imported to mitochondria.

In order to confirm this hypothesis, we generated transgenic *C. elegans* strains expressing AGXT-1 fused to the N-terminus of tagRFP. Considering that previous studies have shown the *in vivo* promoter activity of the *agxt-1* gene in muscle cells [33,34] and the very distinctive mitochondrial tubular pattern of muscle cells [35,36], our construct was expressed in body wall and vulval muscle cells under the control of the *myo-3* promoter. Unfortunately, expression of the full AGXT-1 fused to tagRFP resulted in big clumps of fluorescence, reminiscent of aggregation and distorted mitochondria (data not shown). This could be a consequence of either a non-proper folding of tagRFP and/or the high level of expression of the recombinant protein. To avoid this aggregation issue, we generated additional transgenic strains expressing only the fusion of the N-terminal sequence of AGXT-1 (containing the putative MTS) with tagRFP. We generated two different transgenic strains expressing the first 50 and 100 amino acids of AGXT-1 fused in frame with tagRFP. As mitochondrial marker, we used a transgenic strain expressing a TOMM-20::GFP fusion protein [37,38]. When tagRFP was expressed alone (Fig. 2a), a diffused cytosolic pattern was seen (Fig. 2c), compared with the mitochondrial localization of TOMM-20::GFP protein (Fig. 2b). However, tagRFP fused to either the first 50 or 100 amino acids of AGXT-1 (Fig. 2e–i), was targeted to mitochondria (Fig. 2g–k), as demonstrated by the colocalization with TOMM-20::GFP (Fig. 2h–l). These data confirm that the N-terminus of AGXT-1 encodes a functional MTS, thus reinforcing the idea of AGXT-1 being a mitochondrial enzyme in *C. elegans*.

3.2. AGXT-1 and hAGT1 share overall structure

Taking into account the considerable sequence homology between AGXT-1 and hAGT1, we built a structural homology model of AGXT-1 using the available crystal structure of hAGT1 as a template [24]. Due

```
                    ....|....|....|....|....|....|....|....|....|....|....|....|

C.elegans|gi.5824614   | MISTRFLRPSVSIFGFGIKSSMSSRAPPKALLQDMVVPPRQLFGPGPSNMADSIAETQSR 60
H.sapiens|gi.126522481 | ------------------MASHKLLVTPPKALLKPLSIPNQLLLGPGPSNLPPRIMAAGGL 43
                                            : *     :******: : :* : *:******:   *  : .

C.elegans|gi.5824614   | NLLGHLHPEFVQIMADVRLGLQYVFKTDNKYTFAVSGTGHSGMECAMVNLLEPGDKFLVV 120
H.sapiens|gi.126522481 | QMIGSMSKDMYQIMDEIKEGIQYVFQTRNPLTLVISGSGHCALEAALVNVLEPGDSFLVG 103
                         ::::* :  :: *** ::: *:****:* *  *:.:**:**..:*.*:**:*****.***

C.elegans|gi.5824614   | EIGLWGQRAADLANRMGIEVKKITAPQGQAVPVEDIRKAIADYKPNLVFVCQGDSSTGVA 180
H.sapiens|gi.126522481 | ANGIWGQRAVDIGERIGARVHPMTKDPGGHYTLQEVEEGLAQHKPVLLFLTHGESSTGVL 163
                           *:*****.*:.:*:* .*: :*   *    ::::.:.:*::** *:*: :*:*****

C.elegans|gi.5824614   | QPLETIGDACREHGALFLVDTVASLGGTPFAADDLKVDCVYSATQKVLNAPPGLAPISFS 240
H.sapiens|gi.126522481 | QPLDGFGELCHRYKCLLLVDSVASLGGTPLYMDRQGIDILYSGSQKALNAPPGTSLISFS 223
                         ***: :*: *:.: .*:***:********:  *   :* :**.:**.****** : ****

C.elegans|gi.5824614   | DRAMEKIRNRKQRVASFYFDAIELGNYWGCDGELKRYHHTAPISTVYALRAALSAIAKEG 300
H.sapiens|gi.126522481 | DKAKKKMYSRKTKPFSFYLDIKWLANFWGCDDQPRMYHHTIPVISLYSLRESLALIAEQG 283
                         *:* :*: .** :  ***:*   *.*:**** : : **** *: ::*:** :*: **::*

C.elegans|gi.5824614   | IDESIQRHKDNAQVLYATLKKHGLEPFVVDEKLRLPCLTTVKVPEGVDWKDVAGKMMT-N 359
H.sapiens|gi.126522481 | LENSWRQHREAAAYLHGRLQALGLQLFVKDPALRLPTVTTVAVPAGYDWRDIVSYVIDHF 343
                         ::::* ::*:: *  *:. *:  **: ** *  **** :*** ** * **:*:.. ::

C.elegans|gi.5824614   | GTEIAGGLGATVGKIWRIGTFGINSNSTKIENVVELLSKSIGEKSK--- 405
H.sapiens|gi.126522481 | DIEIMGGLGPSTGKVLRIGLLGCNATRENVDRVTEALRAALQHCPKKKL 392
                           ** **** :.**: *** :* *:.  ::: .*.* *  :: .  *
```

Fig. 1. Protein sequence comparison between nematode AGXT-1 and human hAGT1 protein. AGXT-1 (GI: 5824614) and hAGT1 (GI: 126522481) protein sequence; identical residues are marked as (*), similar residues as (:), residues with similar shapes as (.) and gaps by (-); residues of the active site are highlighted in red, while gaps in both terminal domains are in green.

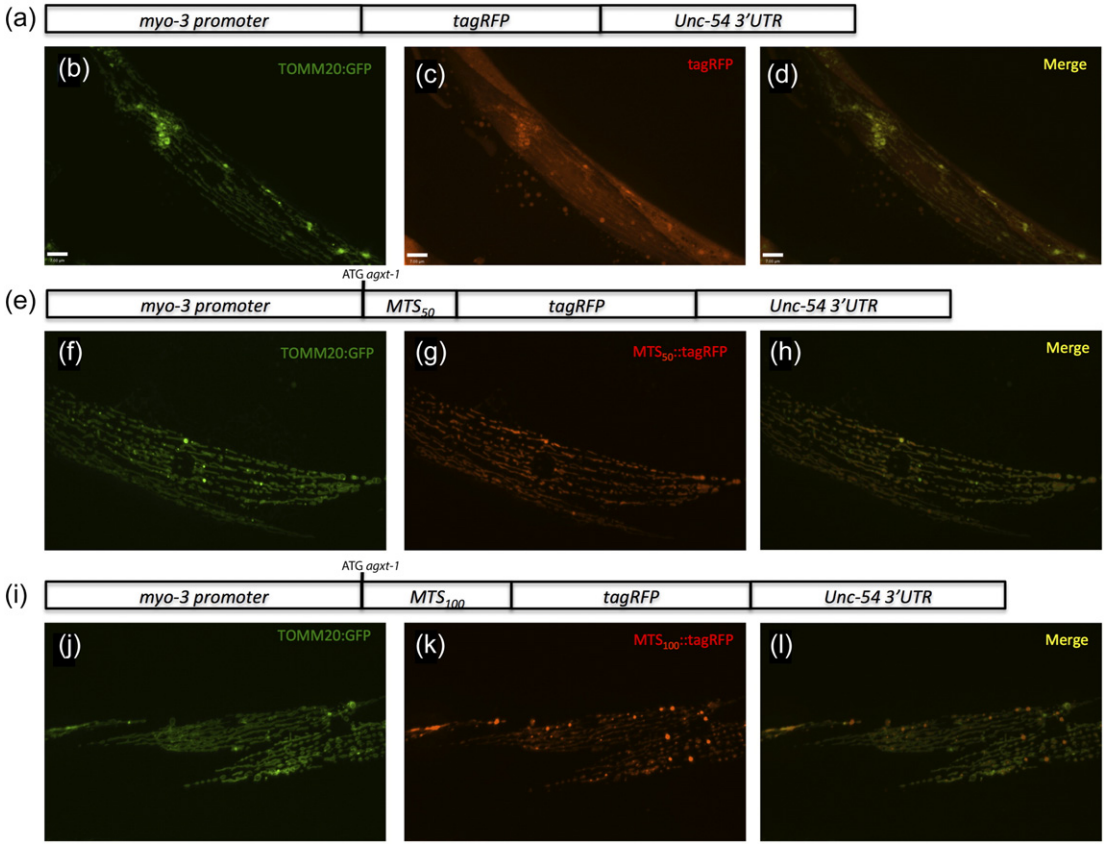

Fig. 2. Mitochondrial localization of AGXT-1. Cartoons representing the DNA constructs used to express tagRFP (a), the first 50 amino acids (e) and the first 100 amino acids (i) of AGXT-1 fused to tagRFP under the control of the *myo-3* promoter along with the *unc-54* 3′-UTR. TOMM-20::GFP expression is found with the typical tubular mitochondrial pattern in muscle cells (b, f and j). When tagRFP is expressed alone, a diffused cytosolic pattern is seen (c) and no colocalization is found with TOMM-20::GFP (d, merge). Fusing the first N-terminal 50 (MTS_{50}) (g) or 100 (MTS_{100}) (k) amino acids of the AGXT-1 to tagRFP targets the protein to mitochondria. The GFP and tagRFP fluorescence now colocalize to the same organelle (h and l, merge).

to the high flexibility of the N-terminus of hAGT1 and substantial sequence differences between the N-terminal domains of both proteins (Fig. 1), we did not include in the structural alignment the first 38 and 23 amino acids of AGXT-1 and hAGT1, respectively. The AGXT-1 model was subsequently refined by energy minimization. The superposition of the obtained AGXT-1 model and the hAGT1 structure predicts that the two proteins share a similar overall conformation and secondary structure composition (Fig. 3a). The binding mode of PLP to AGXT-1 protein appears to be very similar to that of the human enzyme and involves a Schiff base linkage with Lys226, a base stacking hydrophobic interaction between the pyridine ring and the side chain of Trp125, a salt bridge between the N1 of PLP and Asp200, an H-bond of the 3′OH group of PLP and Ser175 and several H-bonds between the phosphate group of the coenzyme and Gln225, Gly99 and His100 (Fig. 3b). Moreover, two interchain contacts of the phosphate group of PLP in hAGT1 with Tyr260 and Thr263 of the neighbouring subunit, are probably held by Tyr277 and Thr280 in AGXT-1.

However, some differences are visible in the active site region and on the protein surface. As for the active site cleft, Ser81 that in hAGT1 is critical for PLP binding [39] is replaced by a threonine residue (Thr98) in AGXT-1. Moreover, Arg360, whose side chain binds the carboxylate group of the substrate in hAGT1 [24], is replaced by Ile377 in AGXT-1 (Fig. 3c), thus leading to a different active site polarity and possibly a different substrate binding mode. In addition, Trp246 and Met259 of hAGT1 are replaced by Glu263 and Arg276 in AGXT-1. As shown in Fig. 3d, these two charged residues could interact by a salt bridge, thus probably stabilizing the interface loop 276–282 comprising the aforementioned Tyr277 and Thr280 residues involved in the binding of the coenzyme. Electrostatic surface map calculations revealed that AGXT-1 would exhibit a higher density and a different distribution of the surface charges with respect to hAGT1 (not shown).

3.3. AGXT-1 is a dimeric PLP-dependent alanine:glyoxylate aminotransferase

To compare the molecular properties of AGXT-1 and hAGT1, both recombinant proteins were expressed in and purified from *E. coli*. Along protein purification, size-exclusion chromatography analyses showed a single peak with similar retention volumes for both proteins and attributable to a dimer (82.6 ml and 84.9 ml in a Superdex™ 200 16/60 for hAGT1 and AGXT-1, respectively). Dynamic light scattering studies also revealed similar hydrodynamic diameters for both proteins (8.1 ± 0.1 nm *vs.* 8.8 ± 0.4 nm, for hAGT1 and AGXT-1, respectively), thus further confirming the dimeric assembly of the two proteins [16,40]. As isolated, both proteins show spectroscopic features corresponding to PLP bound to the active site by a Schiff base with Lys209 in hAGT1 and Lys226 in AGXT-1. The UV–visible absorption and CD spectra of AGXT-1 display a band at 430 nm, which likely reflects the ketoenamine tautomer of the internal Schiff base, and a band at 340 nm, possibly corresponding to enolimine tautomer (Fig. 4 and [6]). After incubation of AGXT-1 with L-alanine, the spectra show almost no signal at 430 nm and a main absorption peak and weak dichroic band at 340 nm (Fig. 4). These signals indicate the formation of the pyridoxamine-5′-phosphate (PMP) form of the coenzyme, thus supporting the proper binding of PLP in the active site of AGXT-1 to take the amino group from the substrate L-alanine. Attempts to remove the coenzyme from the active site of AGXT-1 (to obtain the apo-form)

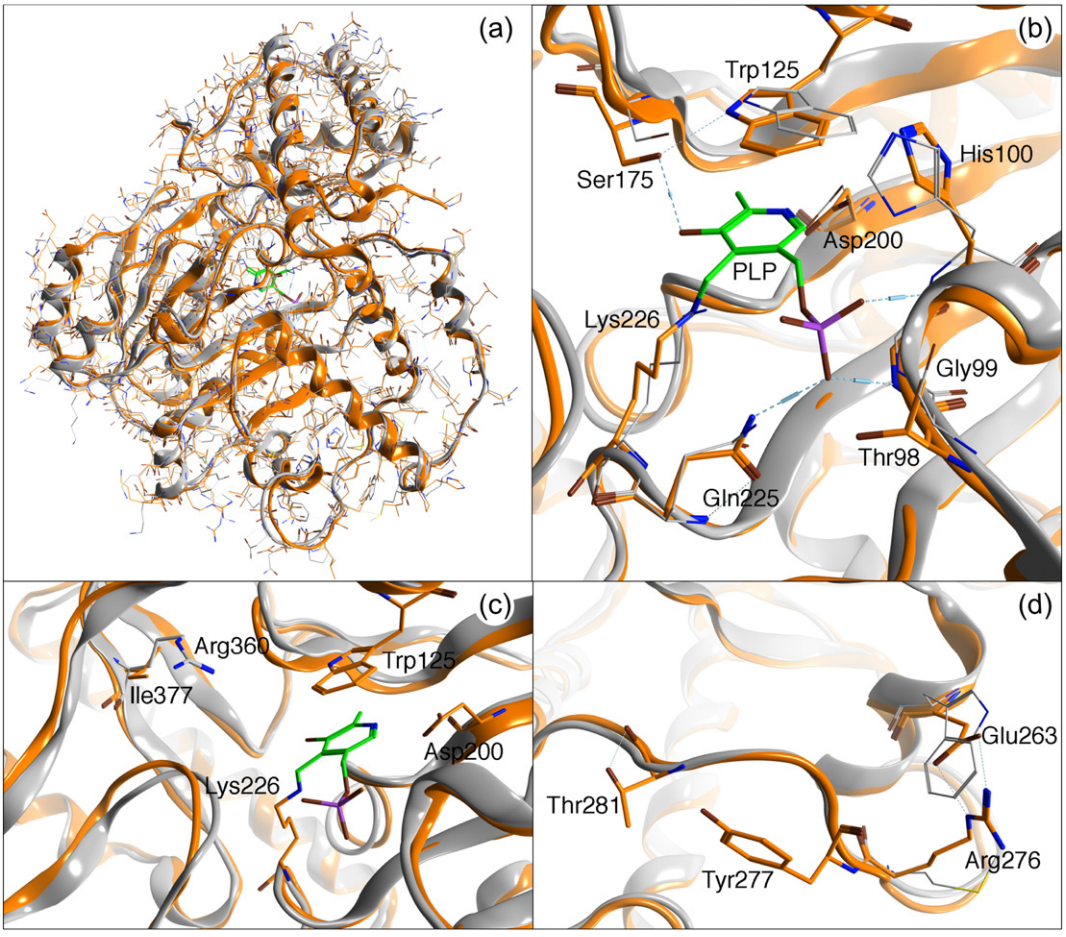

Fig. 3. Structural alignment of the AGXT-1 model with the hAGT1 structure. Structural over imposition of AGXT-1 (orange) and hAGT1 (grey). The two backbones are represented as ribbons and the single residues as sticks. The PLP molecule is represented as green sticks.

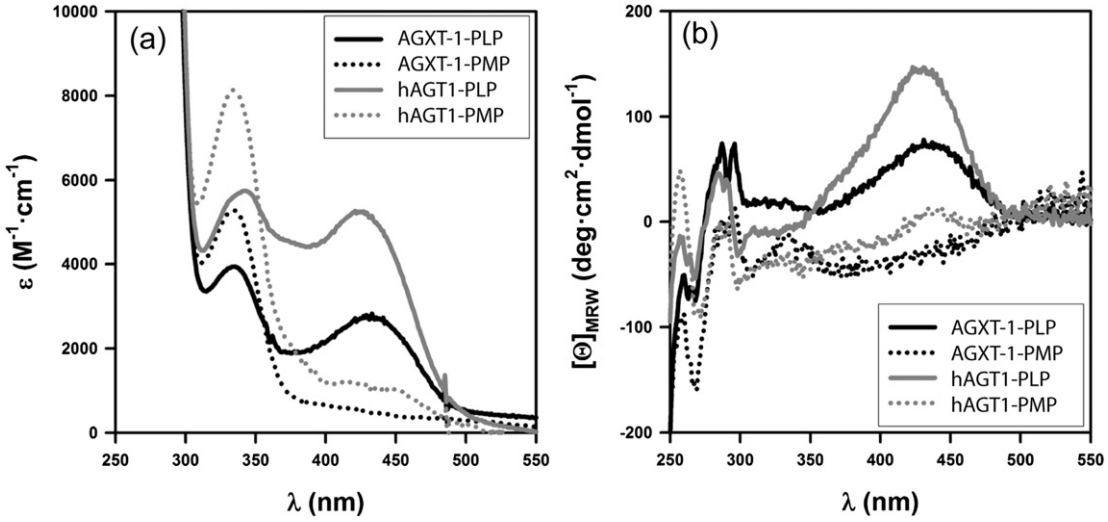

Fig. 4. Near-UV/visible spectroscopic analyses of AGXT-1 and hAGT1 in their PLP-bound forms and in the presence of 0.5 M L-alanine (PMP-forms). (a) Near-UV/visible absorption spectra; (b) Near UV/visible circular dichroism spectra; protein concentration was 20 μM in monomer.

by using the procedure applied for hAGT1 [16,17] yielded a form of AGXT-1 with PMP tightly bound, suggesting a very high affinity and/or very slow dissociation rate of PMP. Further reduction of the pH (below 5.8) resulted in irreversible denaturation of AGXT-1 before the release of the coenzyme, thus preventing a comparison between the apo-form of AGXT-1 and hAGT1. Together, these results suggest that AGXT-1 binds PMP with higher affinity than hAGT1 and/or that the pH value for efficient PMP release is lower for AGXT-1.

Next, the ability of AGXT-1 to catalyse the amino transfer by using the natural substrates of hAGT1 (L-alanine and glyoxylate) was tested (Fig. 5). Activity data were analysed by using a coupled enzyme assay as described for hAGT1 [6,16]. Kinetic parameters for the overall transamination show that AGXT-1 has 5-fold higher activity (V_{max}) than hAGT1 (Table 2), while apparent affinities (K_M) for both substrates are kept in similar ranges. Only the apparent affinity for L-alanine is slightly higher (1.6-fold higher) for AGXT-1 than for hAGT1. These results support a higher catalytic efficiency towards glyoxylate for the nematode enzyme than for the hAGT1. In addition, both proteins show similar dependence of the overall transaminase activity on temperature and pH (Fig. 6). Arrhenius analyses of temperature dependence of transaminase activity reveal an activation energy value of 4.0 ± 0.9 kcal·mol^{-1} for AGXT-1, somewhat higher than for hAGT1 (2.2 ± 1.8 kcal·mol^{-1}) (Fig. 6a). The activity of both enzymes decreases at mild acidic pH (Fig. 6b–c), suggesting similar pattern of protonation states of the active site of both proteins, which could be a sign of similar reaction specificities [41] and environmental pH in their intracellular localization [42].

The large difference in activity between AGXT-1 and hAGT1 towards the alanine:glyoxylate pair prompted us to investigate whether these two enzymes may share similar substrate specificity [6]. To this aim, we determined the specific activity of these enzymes by using glyoxylate or pyruvate as amino acceptors and different natural L-amino acids as amino donors (Fig. 7). When using glyoxylate as amino acceptor, AGXT-1 protein is very specific towards L-alanine showing 300-fold and 130-fold higher activity than for L-serine and L-phenylalanine and no detectable activity towards L-arginine, L-glutamate and L-aspartate (Fig. 7a). Under similar conditions, hAGT1 is somewhat less specific, with 23-fold and 52-fold lower activity towards L-serine and L-arginine and 100-fold and 200-fold lower activity towards L-phenylalanine and L-glutamate (Fig. 7a). Using pyruvate as amino acceptor (Fig. 7b), both enzymes display lower activity towards L-serine than those measured using glyoxylate. Their activities towards L-phenylalanine are comparable, L-arginine is a better substrate for hAGT1 than AGXT-1 and L-glutamate and L-aspartate are poor substrates for both enzymes. Even though some differences exist, these studies support similar substrate

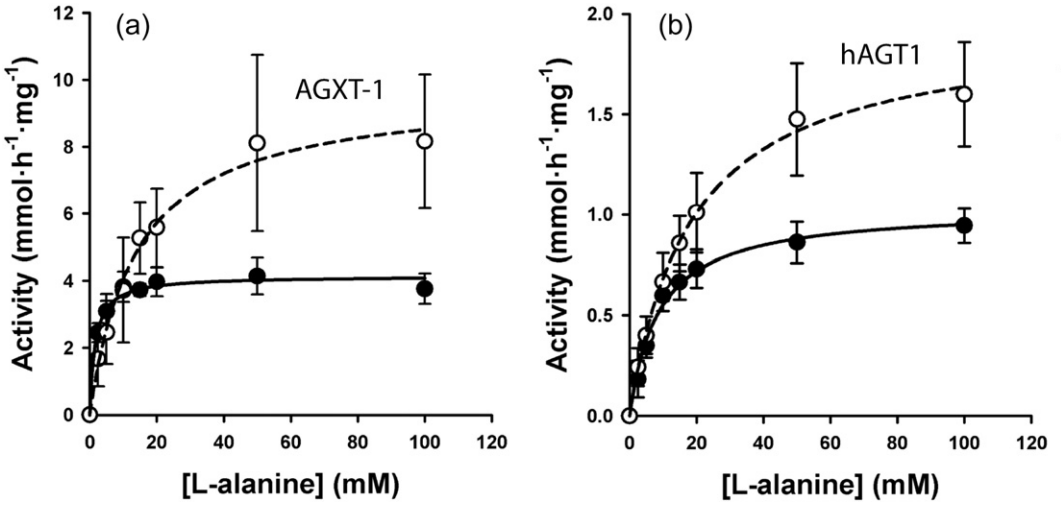

Fig. 5. Enzyme kinetic analyses of AGXT-1 (a) and hAGT1 (b) proteins in the presence of L-alanine and glyoxylate. Experiments were performed at 0.25 mM (closed circles) and 2 mM (open circles) glyoxylate and varying L-alanine concentrations. Lines are global best-fits to an enzyme-substituted kinetic mechanism yielding the kinetic parameters shown in Table 2.

Table 2
Kinetic parameters of the overall transaminase activity for AGXT-1 and hAGT1. Data are mean ± s.d. from global fits using a coupled enzyme assay.

Parameter	AGXT-1	hAGT1
V_{max} (mmol·h^{-1}·mg^{-1})	11.3 ± 0.7	2.2 ± 0.1
$K_{M,alanine}$ (mM)	12 ± 2	20 ± 2
$K_{M,glyoxylate}$ (mM)	0.26 ± 0.05	0.26 ± 0.04

specificities for both proteins and demonstrate that AGXT-1 protein is an alanine:glyoxylate aminotransferase.

3.4. AGXT-1 shows lower resistance towards thermal and chemical denaturation

Thermal denaturation of AGXT-1 was studied by differential scanning calorimetry (DSC). Both AGXT-1 and hAGT1 show a single denaturation transition (Fig. 8a), which is well described by a simple two-state irreversible denaturation model with first-order kinetics (supported by protein concentration independent denaturation transitions [16,17] and data not shown). The denaturation temperature (T_m) of AGXT-1 is about 12 °C lower than that of hAGT1 (Table 3). The lower denaturation enthalpy (ΔH) of AGXT-1 seems to be a consequence of the lower thermal stability of this protein and a strongly temperature dependent ΔH with a theoretical denaturation heat capacity of about 11 kcal·mol^{-1}·K^{-1} (based on the correlations by [43]), thus suggesting that the amount of tertiary structure lost upon thermal denaturation in both enzymes is fairly similar. Due to the kinetic control of thermal denaturation for both enzymes, the DSC analyses can be used to extrapolate the denaturation rate constants to physiological temperatures (inset Fig. 8a). The extrapolated kinetic stability for AGXT-1 towards thermal denaturation at 37 °C is around 200-fold lower than hAGT1 at this temperature (Table 3). However, when we compare the kinetic stability of both proteins at the corresponding physiological temperature (37 °C for

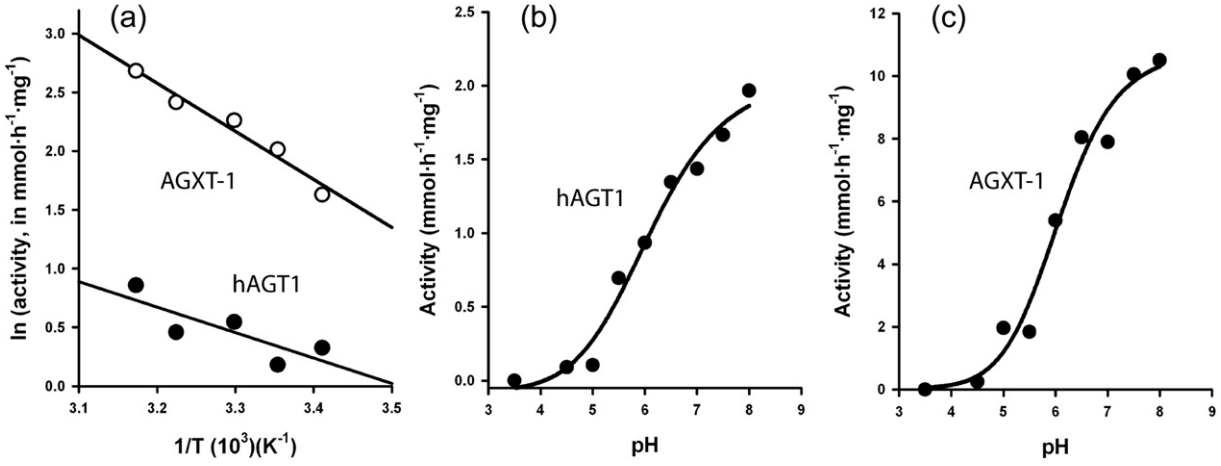

Fig. 6. Temperature- and pH-dependence of the overall transaminase activity for AGXT-1 and hAGT1 proteins. (a) Arrhenius plots for the enzymatic activity of AGXT-1 and hAGT1; (b) and (c) pH-dependence of the enzymatic activity of hAGT1 and AGXT-1, respectively. Activity was measured in the presence of 100 mM L-alanine and 2 mM glyoxylate.

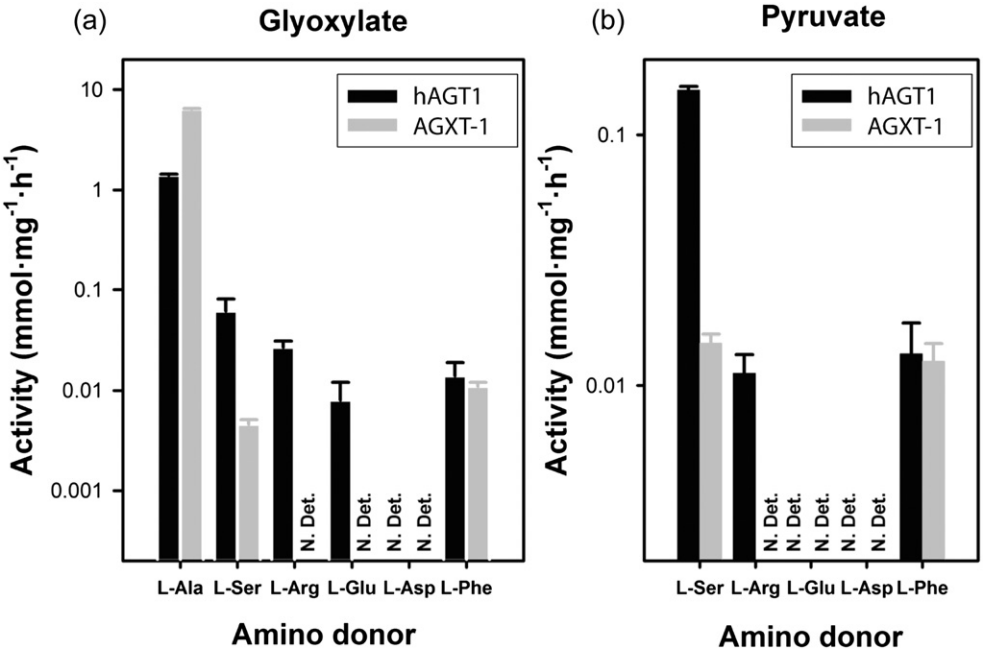

Fig. 7. Substrate specificity of AGXT-1 and hAGT1 towards different amino acids as amino donor using glyoxylate (a) or pyruvate (b) as amino acceptors. The concentration of amino acids was 100 mM and of ketoacids was 2 mM. N.Det. — not detected.

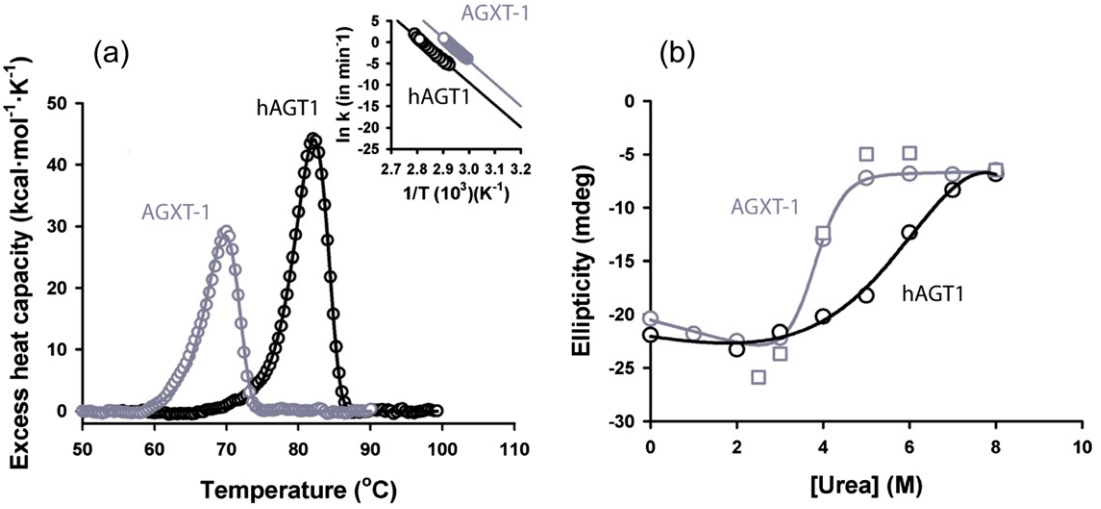

Fig. 8. Stability of AGXT-1 and hAGT1 proteins towards thermal and chemical denaturation. (a) Thermal denaturation profiles of holo AGXT-1 and hAGT1 at 3 °C·min^{-1} and 5 μM protein subunit in 20 mM Na-Hepes, 200 mM NaCl pH 7.4. Lines are best-fits to a two-state irreversible model with first-order kinetics; inset: Arrhenius plots for thermal denaturation kinetics; (b) urea-induced unfolding of holo AGXT-1 and hAGT1 at 5 μM protein subunit in 20 mM Na-Hepes, 200 mM NaCl pH 7.4, 1 mM TCEP at 25 °C. Circles show the results for unfolding, while squares correspond to refolding experiments.

hAGT1 and 20 °C for AGXT-1) the nematode protein is 90-fold more stable than hAGT1.

Urea induced denaturation of AGXT-1 was investigated by Far-UV circular dichroism spectroscopy (Fig. 8b). Denaturation profiles of AGXT-1 and hAGT1 show a single transition and once again, AGXT-1 displays a lower stability with half-denaturation urea concentration of ~3.8 M (AGXT-1) *vs.* ~6 M (hAGT1). The cooperativity of urea-induced unfolding is apparently higher for AGXT-1 than for hAGT1. In contrast to hAGT1 ([44] and data not shown), urea unfolding of AGXT-1 is highly reversible (Fig. 8b squares). This reversibility suggests that, upon chemical denaturation, the refolding pathway of AGXT-1 populates less aggregation-prone intermediate states.

4. Discussion

Glyoxylate is a metabolic intermediary in humans that has to be detoxified mainly by hAGT1 in peroxisomes [2]. Instead, glyoxylate is a key metabolite in *C. elegans* due to the presence of an active glyoxylate cycle [10,12]. The sequencing of *C. elegans* genome predicted a putative ortholog of human *AGXT* gene in the nematode (ORF *T14D7.1*, [9] now renamed to *agxt-1*). However, the product of *agxt-1* gene has not been previously investigated. Here, we have performed a side-by-side comparative study on the molecular properties of AGXT-1 protein in comparison with human hAGT1, showing that AGXT-1 is a functional PLP-dependent enzyme with aminotransferase activity and a higher activity and specificity towards the alanine:glyxoxylate pair than hAGT1. Our results also support that both enzymes are structurally and functionally alike, but show different protein stability and subcellular localization, where AGXT-1 is mitochondrial and hAGT1 is peroxisomal.

Table 3
Thermal denaturation parameters for AGXT-1 and hAGT1. The parameters have been determined from DSC scans using a two-state irreversible denaturation model.

Parameter	AGXT-1	hAGT1[a]
T_m (°C)[b]	69.8	82.1
ΔH (kcal·mol^{-1})[c]	366 ± 11	548 ± 5
E_a (kcal·mol^{-1})[c]	112 ± 15	109 ± 5
$k_{37°C}$ ($k_{20°C}$) (min^{-1})[d]	1.2 · 10^{-7} (7.1 · 10^{-12})	6.4 · 10^{-10}

[a] Data from Mesa-Torres, PLoS One, 2013.
[b] Determined at 3 °C·min^{-1} scan rate.
[c] Mean ± s.d. from three different scan rates.
[d] Kinetic constant rates for irreversible denaturation extrapolated to 37 °C (20 °C).

The mitochondrial localization of AGXT-1 provides important insights into the evolutionary adaptation of AGTs subcellular compartmentalization, and possibly, into its relation with dietary origins of glyoxylate and the molecular origin of mitochondrial mistargeting in PH1. AGT subcellular localization has represented a remarkable conundrum for cell and evolutionary biologists and molecular pathologists. The AGTs peroxisomal localization is attributed to a PTS1 located at the C-terminal domain, while the mitochondrial localization is mainly controlled by the activation of a cryptic MTS in the N-terminal domain that overrides the PTS1 route [1]. Therefore, the *AGXT* gene seems to have evolved to meet dietary requirements, with alternative translation and transcription sites to allow the protein to contain this strong MTS sequence [45]. In most omnivorous mammals the AGT enzyme is distributed in mitochondria or peroxisomes, based on the presence or absence of the MTS, respectively. In carnivorous mammals, the AGT localization is mainly mitochondrial while a selective loss of the MTS is found in herbivorous animals [46]. These evolutionary changes in subcellular distribution of AGT associated with dietary changes have been recently exemplified by sequencing and evolutionary analyses on different bat species with unparalleled dietary diversification [47]. Importantly, hAGT1 contains a very weak MTS, which becomes stronger in the presence of the destabilizing P11L polymorphism and certain pathogenic mutations, that result into mitochondrial mistargeting [16,48]. Unlike the behaviour found along evolution, which seems to define the subcellular targeting of AGT using relatively simple transcriptional and translational mechanisms, mitochondrial mistargeting of hAGT1 seems to depend strongly on the cellular context. For instance, a given single genotype may lead or not to mitochondrial import depending on the cell type and culture conditions [16,49,50] highlighting the important role of molecular chaperones and/or other factors of the protein homeostasis network in the final fate of hAGT1 disease-causing variants [16,17].

Along evolution, enzyme properties are selected to provide appropriate metabolic rates at different physiological temperatures by tuning some structure-function relationships i.e., stability, enzyme activity and ligand affinity [51]. While the physiological temperature of humans is kept constant at 37 °C, the nematode *C. elegans* is an ectotherm organism that can survive between 8 and 27 °C and whose physiology is highly affected by the environmental temperature. The lower denaturation temperature and high catalytic activity of AGXT-1 likely reflects temperature-adaptation [52]. Moreover, the similar apparent affinities for natural substrates of hAGT1 displayed by AGXT-1, suggest

resemblance in substrate concentration or K_M:[substrate] ratio, at their respective organelles [53]. It must be noted that the activity and intracellular turnover of hAGT1 must be tuned to be appropriate at a customarily constant temperature of 37 °C, while the conformational stability of AGXT-1 seems to be adapted to lower temperatures. These results may indicate that the overall stability of different AGT orthologs is optimized to provide an adequate intracellular turnover at optimal growth temperature, which in the case of hAGT1 is severely compromised by disease-associated mutations leading to protein misfolding and mistargeting [2,16,40,54].

The main biological function of hAGT1 is to create a glyoxylate sink in peroxisomes of hepatocytes. In addition, there is a set of proteins that contribute to this human glyoxylate metabolism. According to KEGG (Kyoto Encyclopedia of Genes and Genomes) and REACTOME Pathway Database, these proteins are D-amino acid oxidase (hDAO), hydroxyacid oxidase (hHAO), glyoxylate reductase/hydroxypyruvate reductase (hGRHPR), D-4-hydroxy-2-oxoglutarate aldolase (hHOGA1), alanine:glyoxylate aminotransferase 2 (hAGT2) and lactate dehydrogenase (hLDH) (Fig. 9). Despite the key role of glyoxylate cycle in *C. elegans* [55] (Fig. 9), surprisingly the genome of the nematode encodes orthologous proteins to those already described for the human glyoxylate metabolism, with the only exception of mitochondrial hHOGA1 protein (Table 4). Therefore the main routes of glyoxylate metabolism in humans are expected to work in the nematode, at least to some extent. Some phenotypes have been described by large-scale gene downregulation in *C. elegans*, such as the association of C31C9.2 (ortholog of hGRHPR) [9] with embryonic lethality [56] and slow growing [57], or T09B4.8 (ortholog of hAGT2) linked to a reduction of fat content [58]. However, according to the WormBase Consortium (www.wormbase.org - WS249) no altered lethality, fertility or development has been ascribed to the lack of function of AGXT-1, F41E6.5 (ortholog of hDAO), DAAO1 and LDH-1 proteins. This suggests that the steps of glyoxylate metabolism that are catalysed by these enzymes may not be essential for the normal development and metabolism of the nematode. Nonetheless, the relative contributions of these enzymes to different biochemical pathways requires knowledge on their enzymatic properties and regulation, expression levels and metabolic fluxes, which can be developmental and environmental dependent [59]. Alternatively, there are no orthologous proteins in humans to the key *C. elegans* enzyme ICL-1, although a human malate synthase activity has been detected with unknown biological function [60].

In *C. elegans*, GC bypasses the decarboxylation steps of TCA cycle supplying a net synthesis of 4-carbon compounds and thus supporting gluconeogenesis by incorporating acetyl-CoA (particularly

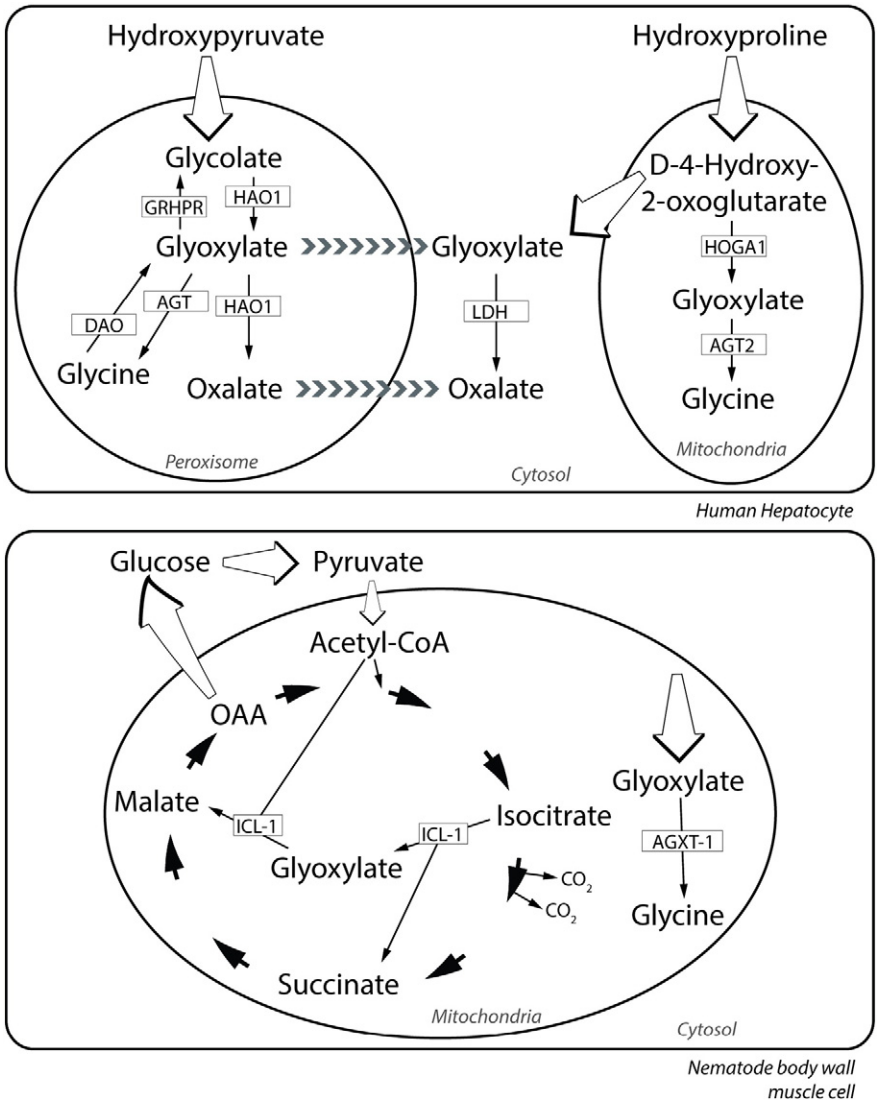

Fig. 9. Main routes of glyoxylate metabolism in human hepatocytes and nematode body wall muscle cells. AGT: alanine:glyoxylate aminotransferase, DAO: D-amino acid oxidase, HAO1: hydroxyacid oxidase, GRHPR: glyoxylate reductase / hydroxypyruvate reductase, HOGA1: D-4-hydroxy-2-oxoglutarate aldolase, AGT2: alanine:glyoxylate aminotransferase 2, LDH: lactate dehydrogenase and ICL-1: bi-functional isocitrate lyase:malate synthase.

Table 4
Orthologous proteins in *C. elegans* found from a BLASTP of human proteins involved in glyoxylate metabolism. GI numbers of protein sequence used are: hAGT-126522481; hDAO-148539837; hHAO-11068137; hGRHPR-6912396; hHOGA-31543060; hAGT2-119576316; hLDH-32693754. n/a, not available. Perox.: peroxisomes; Cyt.: cytosol; Mito.: mitochondria.

H. sapiens			*C. elegans*			
Protein	Residues	Localization	Protein	Residues	Identity	E value
hAGT	392	Perox.	AGXT-1	405	44%	$5 \cdot 10^{-115}$
hDAO	347	Perox.	DAAO1	322	35%	$8 \cdot 10^{-61}$
hHAO	370	Perox.	F41E6.5b	371	46%	$6 \cdot 10^{-115}$
hGRHPR	328	Perox./Cyt.	C31C9.2	322	30%	$1 \cdot 10^{-29}$
hHOGA	327	Mito.	Not found	n/a	n/a	n/a
hAGT2	514	Mito.	T09B4.8	444	53%	$1 \cdot 10^{-165}$
hLDH	332	Cyt.	LDH-1	333	54%	$6 \cdot 10^{-119}$

from β-oxidation of fatty acids in peroxisome and mitochondria) and supplying succinate to TCA cycle and malate to the gluconeogenesis pathway [13,14]. The GC activity is increased during embryogenesis, L1 larvae and dauer diapause, while TCA cycle is increased in the L2, L3 and L4 stages, when energy demands and food intake are increased [14]. The GC and TCA cycles share some enzymatic activities (malate dehydrogenase, citrate synthase and aconitase), while some enzymes, ICL-1 (GC) and isocitrate dehydrogenase (TCA), compete for the same substrate (isocitrate). Therefore the relative activity of these enzymes controls the ratio of carbon flux through both cycles (GC and TCA) [55]. Historically, unlike other nematodes [61], key enzymes of GC in *C. elegans* have been considered to be compartmentalized in glyoxysome-like microbodies by being found in a heavier band (apart from mitochondrial markers) in isopycnic centrifugation [62]. However, it has been recently demonstrated that C-terminal GFP tagged ICL-1 protein co-localizes with mitochondrial dye MitoTracker [63]. This previous notion of a physical separation between GC and TCA enzymes implied either the existence of isoforms of those shared enzymes activities in glyoxysomes or the transportation of metabolites (e.g., isocitrate and succinate) across organelles membranes [64], which was hypothesized to function as a metabolic regulatory mechanism [65]. The existence of a mitochondrial alanine:glyoxylate aminotransferase (AGXT-1) and ICL-1 activities may imply a direct competition of both proteins for glyoxylate as substrate that may participate in carbon flux through TCA and GC cycle pathways. The transamination of glyoxylate into glycine by AGXT-1 could provide an alternative pathway for glyoxylate conversion and also an additional way to modulate levels of glyoxylate in mitochondria, which could otherwise be toxic and may affect the regulation of the TCA cycle by inhibiting enzymes such as ketoglutarate dehydrogenase [66]. In humans, the hAGT1 activity is known to act in the detoxification of glyoxylate within peroxisomes of hepatocytes, while the presence of an active glyoxylate cycle in the nematode opens the possibility of alternative metabolic roles for the AGXT-1 protein. To further characterize the role of AGXT-1 on different metabolic pathways and developmental conditions, a detailed analysis of metabolites in cultures of *icl-1* and *agxt-1* mutants should be approached.

C. elegans is a remarkably useful model system to understand protein folding diseases and their pharmacological correction [67–69]. Our studies advance that the nematode *C.elegans* could be a model for PH1. Although simultaneous inactivation of *agxt-1* and *icl-1* genes does not result in a clear oxalate accumulation (see Table 5), we cannot rule out the possibility of a hyperoxaluric phenotype under the appropriate stress. Alternatively, models expressing disease-associated variants of hAGT1 in *C. elegans* may also provide a convenient *in vivo* platform to explore and dissect the complex protein homeostasis defects associated with PH1-causing mutations.

Table 5
Glyoxylate and oxalate levels in lysates of wild-type and mutant nematode strains grown in the presence of glyoxylate.

Strain	nmol glyoxylate/mg total protein	nmol oxalate/mg total protein
N2 Bristol	2.48	21.8
UGR9 (*agxt-1*)	2.88	35.8
UGR10 (*icl-1*)	2.22	26.9
UGR11 (*agxt-1*; *icl-1*)	3.35	30.2

Transparency document

The Transparency document associated with this article can be found, in online version.

Acknowledgments

We thank Prof. Jose Manuel Sanchez-Ruiz for support. This work was supported by the Spanish Ministry of Science and Innovation (CSD2009-00088, BIO2012-34937 and SAF2011-23933), the Junta de Andalucia (P11-CTS-7187), and the Oxalosis and Hyperoxaluria Foundation (OHF2012 to B.C.). A.L.P. acknowledges a Ramon y Cajal research contract (RyC2009-04147) from the Spanish Ministry of Science and Innovation and the University of Granada. N. M-T acknowledges a FPI predoctoral fellowship from the Spanish Ministry of Science and Innovation. A.C.C. and N.T. were supported by the grant IOS-1353845 from the National Science Foundation (NSF). N.T. acknowledges the Tetelman Fellowship for International Research on the Sciences awarded by Yale University.

References

[1] C.J. Danpure, Variable peroxisomal and mitochondrial targeting of alanine: glyoxylate aminotransferase in mammalian evolution and disease, BioEssays 19 (1997) 317–326, http://dx.doi.org/10.1002/bies.950190409.
[2] E. Salido, A.L. Pey, R. Rodriguez, V. Lorenzo, Primary hyperoxalurias: disorders of glyoxylate detoxification, Biochim. Biophys. Acta 2012 (1822) 1453–1464, http://dx.doi.org/10.1016/j.bbadis.2012.03.004.
[3] P.R.S. Baker, S.D. Cramer, M. Kennedy, D.G. Assimos, R.P. Holmes, Glycolate and glyoxylate metabolism in HepG2 cells, Am. J. Physiol. Cell Physiol. 287 (2004) C1359–C1365, http://dx.doi.org/10.1152/ajpcell.00238.2004.
[4] B. Caplin, Z. Wang, A. Slaviero, J. Tomlinson, L. Dowsett, M. Delahaye, et al., Alanine-glyoxylate aminotransferase-2 metabolizes endogenous methylarginines, regulates NO, and controls blood pressure, Arterioscler. Thromb. Vasc. Biol. 32 (2012) 2892–2900, http://dx.doi.org/10.1161/ATVBAHA.112.254078.
[5] R.N. Rodionov, N. Jarzebska, N. Weiss, S.R. Lentz, AGXT2: a promiscuous aminotransferase, Trends Pharmacol. Sci. 35 (2014) 575–582, http://dx.doi.org/10.1016/j.tips.2014.09.005.
[6] B. Cellini, M. Bertoldi, R. Montioli, A. Paiardini, V.C. Borri, Human wild-type alanine: glyoxylate aminotransferase and its naturally occurring G82E variant: functional properties and physiological implications, Biochem. J. 408 (2007) 39–50, http://dx.doi.org/10.1042/BJ20070637.
[7] E. Oppici, R. Montioli, B. Cellini, Liver peroxisomal alanine:glyoxylate aminotransferase and the effects of mutations associated with primary hyperoxaluria type I: an overview, Biochim. Biophys. Acta 2015 (1854) 1212–1219, http://dx.doi.org/10.1016/j.bbapap.2014.12.029.
[8] C. elegans Sequencing Consortium, Genome sequence of the nematode *C. elegans*: a platform for investigating biology, Science 282 (1998) 2012–2018 (80-).
[9] P.E. Kuwabara, N. O'Neil, The use of functional genomics in *C. elegans* for studying human development and disease, J. Inherit. Metab. Dis. 24 (2001) 127–138.
[10] W.J. Colonna, B.A. McFadden, Isocitrate lyase from parasitic and free-living nematodes, Arch. Biochem. Biophys. 170 (1975) 608–619.
[11] H.L. Kornberg, N.B. Madsen, Synthesis of C4-dicarboxylic acids from acetate by a glyoxylate bypass of the tricarboxylic acid cycle, Biochim. Biophys. Acta 24 (1957) 651–653.
[12] F. Liu, J.D. Thatcher, J.M. Barral, H.F. Epstein, Bifunctional glyoxylate cycle protein of *Caenorhabditis elegans*: a developmentally regulated protein of intestine and muscle, Dev. Biol. 169 (1995) 399–414, http://dx.doi.org/10.1006/dbio.1995.1156.
[13] F.R. Khan, B.A. McFadden, *Caenorhabditis elegans*: decay of isocitrate lyase during larval development, Exp. Parasitol. 54 (1982) 47–54.
[14] W.G. Wadsworth, D.L. Riddle, Developmental regulation of energy metabolism in *Caenorhabditis elegans*, Dev. Biol. 132 (1989) 167–173.
[15] C.N. Pace, F. Vajdos, L. Fee, G. Grimsley, T. Gray, How to measure and predict the molar absorption coefficient of a protein, Protein Sci. 4 (1995) 2411–2423, http://dx.doi.org/10.1002/pro.5560041120.
[16] N. Mesa-Torres, I. Fabelo-Rosa, D. Riverol, C. Yunta, A. Albert, E. Salido, et al., The role of protein denaturation energetics and molecular chaperones in the aggregation and mistargeting of mutants causing primary hyperoxaluria type I, PLoS One 8 (2013) e71963.

[17] A.L. Pey, E. Salido, J.M. Sanchez-Ruiz, Role of low native state kinetic stability and interaction of partially unfolded states with molecular chaperones in the mitochondrial protein mistargeting associated with primary hyperoxaluria, Amino Acids 41 (2011) 1233–1245, http://dx.doi.org/10.1007/s00726-010-0801-2.

[18] E.A. Peterson, H.A. Sober, Preparation of crystalline phosphorylated derivatives of vitamin B6, J. Am. Chem. Soc. 76 (1954) 169–175, http://dx.doi.org/10.1021/ja01630a045.

[19] G. Rumsby, T. Weir, C.T. Samuell, A semiautomated alanine:glyoxylate aminotransferase assay for the tissue diagnosis of primary hyperoxaluria type 1, Ann. Clin. Biochem. 34 (Pt 4) (1997) 400–404.

[20] B. Cellini, M. Bertoldi, C. Borri Voltattorni, Treponema denticola cystalysin catalyzes beta-desulfination of L-cysteine sulfinic acid and beta-decarboxylation of L-aspartate and oxalacetate, FEBS Lett. 554 (2003) 306–310.

[21] J.M. Sánchez-Ruiz, J.L. López-Lacomba, M. Cortijo, P.L. Mateo, Differential scanning calorimetry of the irreversible thermal denaturation of thermolysin, Biochemistry 27 (1988) 1648–1652.

[22] S. Brenner, The Genetics of *Caenorhabditis elegans*, Genetics 77 (1974) 71–94.

[23] C. Mello, A. Fire, DNA transformation, Methods Cell Biol. 48 (1995) 451–482.

[24] X. Zhang, S.M. Roe, Y. Hou, M. Bartlam, Z. Rao, L.H. Pearl, et al., Crystal structure of alanine:glyoxylate aminotransferase and the relationship between genotype and enzymatic phenotype in primary hyperoxaluria type 1, J. Mol. Biol. 331 (2003) 643–652.

[25] W. Neupert, Protein import into mitochondria, Annu. Rev. Biochem. 66 (1997) 863–917, http://dx.doi.org/10.1146/annurev.biochem.66.1.863.

[26] M.G. Claros, P. Vincens, Computational method to predict mitochondrially imported proteins and their targeting sequences, Eur. J. Biochem. 241 (1996) 779–786.

[27] O. Emanuelsson, S. Brunak, G. von Heijne, H. Nielsen, Locating proteins in the cell using TargetP, SignalP and related tools, Nat. Protoc. 2 (2007) 953–971, http://dx.doi.org/10.1038/nprot.2007.131.

[28] A. Motley, M.J. Lumb, P.B. Oatey, P.R. Jennings, P.A. De Zoysa, R.J. Wanders, et al., Mammalian alanine/glyoxylate aminotransferase 1 is imported into peroxisomes via the PTS1 translocation pathway. Increased degeneracy and context specificity of the mammalian PTS1 motif and implications for the peroxisome-to-mitochondrion mistargeting of, J. Cell Biol. 131 (1995) 95–109.

[29] T.G. Knott, G.M. Birdsey, K.E. Sinclair, I.M. Gallagher, P.E. Purdue, C.J. Danpure, The peroxisomal targeting sequence type 1 receptor, Pex5p, and the peroxisomal import efficiency of alanine:glyoxylate aminotransferase, Biochem. J. 352 (Pt 2) (2000) 409–418.

[30] O.I. Petriv, D.B. Pilgrim, R. Rachubinski, a, Titorenko VI. RNA interference of peroxisome-related genes in *C. elegans*: a new model for human peroxisomal disorders, Physiol. Genomics 10 (2002) 79–91, http://dx.doi.org/10.1152/physiolgenomics.00044.2002.

[31] A.M. Motley, E.H. Hettema, R. Ketting, R. Plasterk, H.F. Tabak, *Caenorhabditis elegans* has a single pathway to target matrix proteins to peroxisomes, EMBO Rep. 1 (2000) 40–46, http://dx.doi.org/10.1038/sj.embor.embor626.

[32] F. Sievers, A. Wilm, D. Dineen, T.J. Gibson, K. Karplus, W. Li, et al., Fast, scalable generation of high-quality protein multiple sequence alignments using Clustal Omega, Mol. Syst. Biol. 7 (2011) 539, http://dx.doi.org/10.1038/msb.2011.75.

[33] S.J. McKay, R. Johnsen, J. Khattra, J. Asano, D.L. Baillie, S. Chan, et al., Gene expression profiling of cells, tissues, and developmental stages of the nematode *C. elegans*, Cold Spring Harb. Symp. Quant. Biol. 68 (2003) 159–169.

[34] D. Dupuy, N. Bertin, C.A. Hidalgo, K. Venkatesan, D. Tu, D. Lee, et al., Genome-scale analysis of in vivo spatiotemporal promoter activity in *Caenorhabditis elegans*, Nat. Biotechnol. 25 (2007) 663–668, http://dx.doi.org/10.1038/nbt1305.

[35] B. Meissner, T. Rogalski, R. Viveiros, A. Warner, L. Plastino, A. Lorch, et al., Determining the sub-cellular localization of proteins within *Caenorhabditis elegans* body wall muscle, PLoS One 6 (2011) e19937, http://dx.doi.org/10.1371/journal.pone.0019937.

[36] H. Fares, A.M. van der Bliek, Analysis of membrane-bound organelles, Methods Cell Biol. 107 (2012) 239–263, http://dx.doi.org/10.1016/B978-0-12-394620-1.00008-4.

[37] S.P. Curran, E.P. Leverich, C.M. Koehler, P.L. Larsen, Defective mitochondrial protein translocation precludes normal *Caenorhabditis elegans* development, J. Biol. Chem. 279 (2004) 54655–54662, http://dx.doi.org/10.1074/jbc.M409618200.

[38] O. Billing, G. Kao, P. Naredi, Mitochondrial function is required for secretion of DAF-28/insulin in *C. elegans*, PLoS One 6 (2011) e14507, http://dx.doi.org/10.1371/journal.pone.0014507.

[39] R. Montioli, A. Roncador, E. Oppici, G. Mandrile, D.F. Giachino, B. Cellini, et al., S81 L and G170R mutations causing primary hyperoxaluria type I in homozygosis and heterozygosis: an example of positive interallelic complementation, Hum. Mol. Genet. (2014)http://dx.doi.org/10.1093/hmg/ddu329.

[40] B. Cellini, R. Montioli, C.B. Voltattorni, Human liver peroxisomal alanine:glyoxylate aminotransferase: characterization of the two allelic forms and their pathogenic variants, Biochim. Biophys. Acta 2011 (1814) 1577–1584, http://dx.doi.org/10.1016/j.bbapap.2010.12.005.

[41] M.D. Toney, Controlling reaction specificity in pyridoxal phosphate enzymes, Biochim. Biophys. Acta 2011 (1814) 1407–1418, http://dx.doi.org/10.1016/j.bbapap.2011.05.019.

[42] P. Chan, J. Warwicker, Evidence for the adaptation of protein pH-dependence to subcellular pH, BMC Biol. 7 (2009) 69, http://dx.doi.org/10.1186/1741-7007-7-69.

[43] A.D. Robertson, K.P. Murphy, Protein structure and the energetics of protein stability, Chem. Rev. 97 (1997) 1251–1268.

[44] B. Cellini, A. Lorenzetto, R. Montioli, E. Oppici, C.B. Voltattorni, Human liver peroxisomal alanine:glyoxylate aminotransferase: different stability under chemical stress of the major allele, the minor allele, and its pathogenic G170R variant, Biochimie 92 (2010) 1801–1811, http://dx.doi.org/10.1016/j.biochi.2010.08.005.

[45] G.M. Birdsey, J. Lewin, A.A. Cunningham, M.W. Bruford, C.J. Danpure, Differential enzyme targeting as an evolutionary adaptation to herbivory in carnivora, Mol. Biol. Evol. 21 (2004) 632–646, http://dx.doi.org/10.1093/molbev/msh054.

[46] C.J. Danpure, P. Fryer, P.R. Jennings, J. Allsop, S. Griffiths, A. Cunningham, Evolution of alanine:glyoxylate aminotransferase 1 peroxisomal and mitochondrial targeting. A survey of its subcellular distribution in the livers of various representatives of the classes Mammalia, Aves and Amphibia, Eur. J. Cell Biol. 64 (1994) 295–313.

[47] Y. Liu, H. Xu, X. Yuan, S.J. Rossiter, S. Zhang, Multiple adaptive losses of alanine-glyoxylate aminotransferase mitochondrial targeting in fruit-eating bats, Mol. Biol. Evol. 29 (2012) 1507–1511, http://dx.doi.org/10.1093/molbev/mss013.

[48] P.E. Purdue, J. Allsop, G. Isaya, L.E. Rosenberg, C.J. Danpure, Mistargeting of peroxisomal L-alanine:glyoxylate aminotransferase to mitochondria in primary hyperoxaluria patients depends upon activation of a cryptic mitochondrial targeting sequence by a point mutation, Proc. Natl. Acad. Sci. U. S. A. 88 (1991) 10900–10904.

[49] A. Santana, E. Salido, A. Torres, L.J. Shapiro, Primary hyperoxaluria type 1 in the Canary Islands: a conformational disease due to I244T mutation in the P11L-containing alanine:glyoxylate aminotransferase, Proc. Natl. Acad. Sci. U. S. A. 100 (2003) 7277–7282, http://dx.doi.org/10.1073/pnas.1131968100.

[50] S. Fargue, J. Lewin, G. Rumsby, C.J. Danpure, Four of the most common mutations in primary hyperoxaluria type 1 unmask the cryptic mitochondrial targeting sequence of alanine:glyoxylate aminotransferase encoded by the polymorphic minor allele, J. Biol. Chem. 288 (2013) 2475–2484, http://dx.doi.org/10.1074/jbc.M112.432617.

[51] G.N. Somero, Adaptation of enzymes to temperature: searching for basic "strategies", Comp. Biochem. Physiol. B Biochem. Mol. Biol. 139 (2004) 321–333, http://dx.doi.org/10.1016/j.cbpc.2004.05.003.

[52] G.N. Somero, Proteins and temperature, Annu. Rev. Physiol. 57 (1995) 43–68, http://dx.doi.org/10.1146/annurev.ph.57.030195.000355.

[53] G.N. Somero, Temperature adaptation of enzymes: biological optimization through structure-function comprimises, Annu. Rev. Ecol. Syst. 9 (1978) 1–29.

[54] E. Oppici, R. Montioli, A. Lorenzetto, S. Bianconi, C. Borri Voltattorni, B. Cellini, Biochemical analyses are instrumental in identifying the impact of mutations on holo and/or apo-forms and on the region(s) of alanine:glyoxylate aminotransferase variants associated with primary hyperoxaluria type I, Mol. Genet. Metab. 105 (2012) 132–140, http://dx.doi.org/10.1016/j.ymgme.2011.09.033.

[55] V.B. O'Riordan, A.M. Burnell, Intermediary metabolism in the dauer larva of the nematode *Caenorhabditis elegans* — II. The glyoxylate cycle and fatty-acid oxidation, Comp. Biochem. Physiol. B Biochem. Mol. Biol. 95 (1990) 125–130.

[56] I. Maeda, Y. Kohara, M. Yamamoto, A. Sugimoto, Large-scale analysis of gene function in *Caenorhabditis elegans* by high-throughput RNAi, Curr. Biol. 11 (2001) 171–176.

[57] M. Hanazawa, M. Mochii, N. Ueno, Y. Kohara, Y. Iino, Use of cDNA subtraction and RNA interference screens in combination reveals genes required for germ-line development in *Caenorhabditis elegans*, Proc. Natl. Acad. Sci. U. S. A. 98 (2001) 8686–8691, http://dx.doi.org/10.1073/pnas.141004698.

[58] K. Ashrafi, F.Y. Chang, J.L. Watts, A.G. Fraser, R.S. Kamath, J. Ahringer, et al., Genome-wide RNAi analysis of *Caenorhabditis elegans* fat regulatory genes, Nature 421 (2003) 268–272, http://dx.doi.org/10.1038/nature01279.

[59] B.P. Braeckman, K. Houthoofd, J.R. Vanfleteren, Intermediary metabolism, WormBook 1–24 (2009)http://dx.doi.org/10.1895/wormbook.1.146.1.

[60] L. Strittmatter, Y. Li, N.J. Nakatsuka, S.E. Calvo, Z. Grabarek, V.K. Mootha, CLYBL is a polymorphic human enzyme with malate synthase and beta-methylmalate synthase activity, Hum. Mol. Genet. (2014)http://dx.doi.org/10.1093/hmg/ddt624.

[61] H. Rubin, R.N. Trelease, Subcellular localization of glyoxylate cycle enzymes in *Ascaris suum* larvae, J. Cell Biol. 70 (1976) 374–383.

[62] T.R. Patel, B.A. McFadden, Particulate isocitrate lyase and malate synthase in *Caenorhabditis elegans*, Arch. Biochem. Biophys. 183 (1977) 24–30.

[63] C. Erkut, V.R. Gade, S. Laxman, T.V. Kurzchalia, The glyoxylate shunt is essential for desiccation tolerance in *C. elegans* and budding yeast, Elife (2016) 5, http://dx.doi.org/10.7554/eLife.13614.

[64] M. Kunze, I. Pracharoenwattana, S.M. Smith, A. Hartig, A central role for the peroxisomal membrane in glyoxylate cycle function, Biochim. Biophys. Acta 2006 (1763) 1441–1452, http://dx.doi.org/10.1016/j.bbamcr.2006.09.009.

[65] R. Bolla, B.M. Zuckerman, et al., Nematode energy metabolism. Nematodes as Biol Model, Aging Other Model Syst. 2 (1980) 165–192.

[66] A. Adinolfi, R. Moratti, S. Olezza, A. Ruffo, Control of the citric acid cycle by glyoxylate. The mechanism of inhibition of oxoglutarate dehydrogenase, isocitrate dehydrogenase and aconitate hydratase, Biochem. J. 114 (1969) 513–518.

[67] B. Calamini, R.I. Morimoto, Protein homeostasis as a therapeutic target for diseases of protein conformation, Curr. Top. Med. Chem. 12 (2012) 2623–2640.

[68] M.C. Silva, S. Fox, M. Beam, H. Thakkar, M.D. Amaral, R.I. Morimoto, A genetic screening strategy identifies novel regulators of the proteostasis network, PLoS Genet. 7 (2011) e1002438, http://dx.doi.org/10.1371/journal.pgen.1002438.

[69] M.O. Casanueva, A. Burga, B. Lehner, Fitness trade-offs and environmentally induced mutation buffering in isogenic *C. elegans*, Science 335 (2012) 82–85, http://dx.doi.org/10.1126/science.1213491.